

# CHARACTERIZATION OF LARGE STRUCTURAL VARIATION USING LINKED-READS

A THESIS SUBMITTED TO  
THE GRADUATE SCHOOL OF ENGINEERING AND SCIENCE  
OF BILKENT UNIVERSITY  
IN PARTIAL FULFILLMENT OF THE REQUIREMENTS FOR  
THE DEGREE OF  
MASTER OF SCIENCE  
IN  
COMPUTER ENGINEERING

By  
Fatih Karaođlanođlu  
Aug 2018

Characterization of Large Structural Variation Using Linked-Reads

By Fatih Karaođlanođlu

Aug 2018

We certify that we have read this thesis and that in our opinion it is fully adequate, in scope and in quality, as a thesis for the degree of Master of Science.

---

Can Alkan(Advisor)

---

Uđur Gdkbay

---

Engin Demir

Approved for the Graduate School of Engineering and Science:

---

Ezhan Karařan  
Director of the Graduate School

# ABSTRACT

## CHARACTERIZATION OF LARGE STRUCTURAL VARIATION USING LINKED-READS

Fatih Karaođlanođlu

M.S. in Computer Engineering

Advisor: Can Alkan

Aug 2018

Many algorithms aimed at characterizing genomic structural variation (SV) have been developed since the inception of high-throughput sequencing. However, the full spectrum of SVs in the human genome is not yet assessed. Most of the existing methods focus on discovery and genotyping of deletions, insertions, and mobile elements. Detection of balanced SVs with no gain or loss of genomic segments (e.g. inversions) is particularly a challenging task. Long read sequencing has been leveraged to find short inversions but there is still a need to develop methods to detect large genomic inversions. Furthermore, currently there are no algorithms to predict the insertion locus of large interspersed segmental duplications.

Here we propose novel algorithms to characterize large (>40Kbp) interspersed segmental duplications and (>80Kbp) inversions using Linked-Read sequencing data. Linked-Read sequencing provides long range information, where Illumina reads are tagged with barcodes that can be used to assign short reads to pools of larger (30-50 Kbp) molecules. Our methods rely on split molecule sequence signature that we have previously described. Similar to the split read, split molecules refer to large segments of DNA that span an SV breakpoint. Therefore, when mapped to the reference genome, the mapping of these segments would be discontinuous. We redesign our earlier algorithm, VALOR, to specifically leverage Linked-Read sequencing data to discover large inversions and characterize interspersed segmental duplications. We implement our new algorithms in a new software package, called VALOR2.

*Keywords:* Structural Variation, Segmental Duplication, Inversion, Linked Reads.

## ÖZET

# BÜYÜK YAPISAL VARYASYONLARIN BAĞLI OKUMALAR KULLANILARAK KARAKTERİZE EDİLMESİ

Fatih Karaođlanođlu

Bilgisayar Mühendisliđi, Yüksek Lisans

Tez Danışmanı: Can Alkan

Ađustos 2018

Yüksek verimli okuma cihazlarının gelişmesiyle yapısal varyasyonların keşfi için birçok algoritma geliştirilmiştir. Ama insan genomundaki YV'ların birçođu henüz belirlenememiştir. Mevcut metotlar delesyon, insersiyon ve mobil elemanlar üzerinde yoğunlaşmaktadır. Dengeli, DNA miktarını deđiştirmeyen varyasyonların tespiti zor bir problemdir. Uzun okuma teknolojileri ile birlikte kısa inversiyonların bulunması mümkün olduysa da, büyük genomik inversiyonların keşfi için yeni metodların geliştirilmesi gerekmektedir. Dahası, şu an büyük segmental duplikasyonların insersiyon lokusunu tahmin eden bir algoritma bulunmamaktadır.

Bu tezde bađlı okuma teknolojilerini kullanarak ardışık olmayan segmental duplikasyonların ve inversiyonların karakterizasyonu için özgün algoritmalar öne sürüyoruz. Bađlı okuma teknolojisi Illumina okumalarını barkodlar ile işaretleyerek uzun mesafe bilgisi sağlamaktadır. Tezdeki metotlar ayırık okuma sinyallerine benzeyen ayırık molekül sinyallerine dayanmaktadır. Ayırık moleküller varyasyon kesim noktalarına denk gelen ve bu nedenle referansa hizalandığında bölünen moleküllerdir. Daha önce Havuzlanmış Klon Dizileme yöntemi için tasarlanmış olan VALOR algoritmasını, bađlı okumalar ile ardışık olmayan segmental duplikasyonları ve inversiyonları bulmak için yeniden tasarladık. Bu yeni algoritmayı, VALOR2 adıyla yeni bir yazılım paketinde uyguluyoruz.

*Anahtar sözcükler:* Yapısal Varyasyon, Segmental Duplikasyon, İnvrsiyon, Bađlı Okumalar.

## Acknowledgements

First and foremost I would like to express my sincerest gratitude to my supervisor, Asst. Prof. Can Alkan, for his continuous support for my graduate studies.

I would like to express my gratitude to my thesis committee: Prof. Uğur Gdkbay and Asst. Prof. Engin Demir.

I would like to thank current and former members of Bilkent Bioinformatics and Computational Genomics Group: Fatma Kahveci, Mohammed Alser, Arda Sylev, Halil İbrahim Özeran, Alim Gkkaya, Ezgi Ebren, Balanur İen, Tuğba Doğan, Zlal Bingl, Marzieh Eslami Rasekh and Can Fırtına.

I would like to thank our collaborators Iman Hajirasouliha and Camir Ricketts from Weill Cornell.

I acknowledge TBİTAK 215E172 grant for the financial support of this project.

Last but not least, I would like to my thank family: Nurettin, Serpil and Gksu Karaođlanođlu, for their endless love, support and patience.

# Contents

- 1 Introduction** **1**
- 1.1 Background Information . . . . . 2
- 1.1.1 Sequencing . . . . . 2
- 1.1.2 Structural Variation . . . . . 5
- 1.1.3 Sequencing Signatures to Detect SVs . . . . . 6
- 1.1.4 Currently available structural variation discovery tools . . . . . 7
- 2 VALOR<sub>2</sub> Algorithm to Discover Large SVs using Linked-Reads** **9**
- 2.1 Motivation . . . . . 9
- 2.2 Challenge . . . . . 10
- 2.3 Linked-Read data . . . . . 12
- 2.4 Mapping linked-reads . . . . . 12
- 2.5 Processing alignments . . . . . 12
- 2.5.1 Determining read fragment size distribution parameters . . . . . 12

2.5.2	Loading and grouping reads . . . . .	13
2.6	Recovering molecules . . . . .	13
2.6.1	Molecule depth signature . . . . .	15
2.7	Split molecule discovery . . . . .	16
2.8	Matching split molecules . . . . .	17
2.9	Filtering predictions with Illumina read pair signatures . . . . .	18
2.10	Clustering predictions . . . . .	18
2.10.1	Constructing SV graph . . . . .	19
2.10.2	Quasi-clique formulation to predict SVs . . . . .	21
<b>3</b>	<b>Results</b>	<b>23</b>
3.1	Simulated data . . . . .	23
3.1.1	Linked-Read simulation . . . . .	23
3.1.2	Inserted variants . . . . .	24
3.1.3	Simulated results and comparison with other methods . . . . .	24
3.2	Real data . . . . .	25
3.2.1	NA12878 . . . . .	25
3.2.2	CHM1 . . . . .	27
<b>4</b>	<b>Discussion and Future Work</b>	<b>29</b>

4.1	Works in progress . . . . .	30
4.1.1	Deletion discovery . . . . .	30
4.1.2	Inter-chromosomal events . . . . .	31
4.2	Future directions . . . . .	33
4.2.1	Structural variation discovery on tumor samples . . . . .	33
4.2.2	Resolving overlapping events . . . . .	33
4.2.3	Expanding the range of predictions . . . . .	33
<b>A</b>	<b>Glossary</b>	<b>44</b>
<b>B</b>	<b>Data</b>	<b>45</b>
<b>C</b>	<b>Code</b>	<b>46</b>



# List of Figures

- 2.1 Read pair signatures for a) inversion, b) interspersed inverted duplication. Note that both variants show ++ and – read-pair signatures. . . . . 11
- 2.2 Molecule depth histogram of NA12878 in chr16 of non-zero bins. Data from [1, 2] . . . . . 15
- 2.3 Split molecule and read pair sequence signatures used in VALOR<sub>2</sub>. a) Inversion, b) interspersed duplication in direct orientation, c) inverted duplication. In each case, the large molecules that span the SV breakpoints are split into two mapped regions. Note that, it is not possible to determine the mapped strand of the split molecules shown here. From the perspective of the reference genome (i.e., mapping), A,B,C,D are defined as *submolecules*, A/B and C/D pairs are *candidate splits*, and A/B-C/D quadruple is a *split molecule pair*. . . . . 17
- 2.4 Asymmetric variations will have split molecule signatures for a) forward copy, b) backward copy direct interspersed duplications. 18
- 2.5 a) SV subgraph of a variant with low mapping ambiguity around the breakpoints. b) SV subgraph of a variant with breakpoints on highly repeated regions. c) SV subgraph of two heterozygous overlapping variants (from simulated data) . . . . . 22

3.1	Comparison of the inversion predictions ( $> 80$ Kb) by VALOR <sub>2</sub> , Long Ranger, DELLY, and LUMPY in the NA12878 genome. . . . .	27
3.2	Intersection of all inversions reported by InvFEST (validated or predicted) with VALOR <sub>2</sub> predictions on CHM1 genome. . . . .	27
4.1	Split molecule and read pair signature of a deletion. . . . .	30
4.2	Split molecule and read pair signature of translocation. Where a segment of DNA is copied from chromosome B to A. . . . .	31
4.3	a and b are molecules with the same barcode in different chromosomes. c is a discordant read pair with one end near a other end near b. We allow gaps between reads and molecules to cover for low coverage. We allow overlaps to be robust to repeats. . . . .	32
4.4	A model to discover smaller duplications, where split molecule information is lost due to small size of the duplication. We can look for discordant read pairs which share barcodes with the molecules around the target. AB and CD molecules are on the duplication, B and C are lost due to low coverage. . . . .	34

# List of Tables

1.1	Read pair signatures and corresponding structural variants. for $+-$ signature to be discordant, distance between read pairs should be larger than $\mu + 3\sigma$ . . . . .	6
3.1	Simulation statistics as generated by VarSim. . . . .	24
3.2	Prediction performance evaluation using simulated structural variants. . . . .	25
3.3	Inversion prediction performance evaluation in the NA12878 genome using InvFEST database. . . . .	26
3.4	Segmental duplications predicted in the NA12878 genome using VALOR <sub>2</sub> . . . . .	28
4.1	Prediction performance evaluation using simulated deletions. . . . .	30
4.2	Read pair signatures and corresponding interchromosomal structural variants. Each pair should map to different chromosomes . . . . .	32

# Chapter 1

## Introduction

Human genome consists of 3 billion base pairs represented with a 4-letter alphabet ( $\Sigma = \{A, C, G, T\}$ ), that correspond to chemical bases; Adenine, Cytosine, Guanine and Thymine. Human genome is highly repetitive. Common repeats make up 50%, segmental duplications make up 5% of the human genome. Humans share 99.9% of their genetic material with other humans, remaining 0.1% is what makes us different. This difference is caused by a variety of genetic events that come in different size and organization. Single nucleotide polymorphisms (SNPs) are the changes of a single base pair of the DNA. Indels are insertions and deletions of base pairs that are smaller than 50 base pairs. Indels and SNPs are the most common genetic events that make up the genetic variation and they are fairly easy to detect. Events that span more than 50 base pairs are called structural variations (SVs) and their length can be as much as millions of base pairs [3]. SVs can be classified into copy number variations (CNVs) and balanced rearrangements. Copy number variations are the variations that change the amount of DNA and can be listed as insertions, deletions, tandem and interspersed duplications. Balanced rearrangements are inversions and translocations. Since they do not change the amount of DNA in the genome, it is not possible to detect balanced rearrangements with methods that utilize read depth (See Subsection 1.1.3.3 for details).

## 1.1 Background Information

### 1.1.1 Sequencing

Sequencing is the process of converting DNA into string of letters. It allows us to read genomes of the organisms. There are several approaches of sequencing, each with its own limitations. We describe some of the sequencing technologies below.

#### 1.1.1.1 Sanger sequencing

For almost 40 years Sanger sequencing [4] also known as chain termination method was the go to method for sequencing. In this method, we start with amplified single stranded DNA fragments and we attach a primers to a known sequence to ensure in the following steps each copy starts at the same position. Then, four vessels are prepared containing DNA polymerase, free nucleotides and a single type of nucleotide (one type for each vessel) lacking an oxygen atom, which stops the synthesis when attached. Then these fragments are sorted by their length/weight using electrical current. Since start positions of each fragment are equal, bases will be identified by their order.

In a 2014 review [5] cost of Sanger sequencing stated to be  $\approx$  \$500/Mb. If we assume cost came down following the Moore's Law, today  $1\times$  coverage of whole human genome will cost  $\approx$  \$40000. While Sanger sequencing is able to generate long reads with low error rate, high cost of the procedure compared to high throughput sequencing methods makes it undesirable for whole genome sequencing. However, it is still useful for smaller projects and validation of the new sequencing methods.

### **1.1.1.2 Human Genome Project**

Human Genome Project aimed to create a reference for the human genome. It launched in 1990 and completed in 2003. It is a consensus gathered from 7-8 individuals, 71% belonging to one person. It covers 99% of the human genome with 99% accuracy (excluding centromeres and telomeres). Cost of Human Genome Project was around \$3 Billion. It is still being updated by including more individuals and refining repeat and gap regions. Latest version, GRCh38 was released in 2013.

### **1.1.1.3 High Throughput Sequencing**

Since their inception, High Throughput Sequencing (HTS) technologies are widely used to discover SNPs, indels and various types of structural variation, [6, 7, 8, 9, 10, 11, 12]. they can be broadly classified as short read sequencing and long read sequencing techniques.

#### **Short read sequencing**

DNA is cut into small pieces and fragments that are in a predetermined size range are selected( $\approx 500$  bp for Illumina platform). These fragments are amplified by polymerase chain reaction (PCR). Afterwards, bases are detected from both ends of these fragments by attaching fluorescently labeled bases with DNA polymerase and capturing the emitted lights unique to each type of base. This method can sequence up to 150 bp with high accuracy, but its quality deteriorates for longer read lengths. Produced by various Illumina sequencing platforms, short reads offer very low error rate for a relatively low price. However, short read lengths makes them less effective at the complex, repetitive regions of the genome [13, 14].

#### **Long read sequencing**

There are two commonly used approaches to long read sequencing, developed by Pacific Biosciences (PacBio) and Oxford Nanopore Technologies (ONT).

PacBio SMRT platform sequences DNA by observing DNA polymerase while it replicates the DNA fragments. Similar to Illumina sequencing, this is done by observing the fluorescent lights emitted. However instead of fluorescent bases, PacBio uses fluorescent phosphates. With this approach, fluorescent lights are removed when bases attach fragment, thus allowing sequencing of whole fragment. Errors are indel dominated, where runaway bases entering the detection zone causes false insertions and inconsistencies with the polymerase speed cause false deletion errors.

Oxford Nanopore sequencers work by observing the disruptions on the electrical current, while DNA fragments passes through a pore. Observed electrical signals then identified using a recurrent neural network. Errors of Nanopore caused by varying passing speed of the fragments through pores and electrical disruptions caused by adjacent bases.

While they can generate long reads, which are useful at interpretation of complex regions of the human genome, their high error rate and relative high cost are prohibitive factors. Despite their high error rate, they are shown to be useful at the characterization of complex structural variants [15, 16, 17, 18].

### **Linked-read sequencing**

Recently Linked-Read sequencing methods such as the 10x Genomics system (10xG) were introduced as an alternative method to generate highly accurate Illumina short reads data with additional long-range information [19]. In the 10xG system, large DNA molecules (typically 10-100 Kbp) are barcoded and randomly separated into over a million partitions (here we term these partitions “pools”). Each pool contains roughly 2-30 large molecules. These pools are then sequenced at very low coverage ( $\sim 0.1X$ ) using the standard Illumina platform. Shared barcodes among Illumina read pairs show them as generated from the same pool. Since each pool is diluted to contain only a very small fraction of the input DNA, the probability of barcode collision is negligible [20]. For example,

assuming 20 molecules per pool and an average size of 30 Kbp per molecule, each pool on average contains only  $\frac{1}{5,000}$  of the haploid human genome. Linked-Reads then can be used to “reconstruct” large molecules that originate from the same haplotype. Furthermore, Linked-Read sequencing makes it possible to obtain very high physical coverage with the cost of generating moderate sequence coverage data<sup>1</sup>.

The ability of extracting long range information from accurate and inexpensive but short read sequencing data makes Linked-Read sequencing attractive for various applications. It has been used for genome scaffolding [21], haplotype-aware assembly [19, 22, 23], metagenomics [24], single cell transcriptome profiling [25, 26] and regulatory network clustering [27], haplotype phasing [19, 22, 28], and genome structural variation discovery [29, 30, 31, 20].

Linked-Read techniques for genomic structural variation discovery include VALOR [29], Long Ranger [30] and GROCSVs [31].

### 1.1.2 Structural Variation

1000 Genomes Project defines alterations in the DNA that affect more than 50 base pairs as structural variation [32]. Structural variation can be examined in two main categories, copy number variations and balanced rearrangements. Deletions, insertions and duplications are classified as copy number variations. Inversions and translocations are balanced rearrangements. Copy number variations change amount of DNA in the genome, while balanced rearrangements do not influence it. Also, structural variations can involve a single chromosome or a pair of chromosomes, called intrachromosomal and interchromosomal events respectively. Segmental duplications and translocations can be either intrachromosomal or interchromosomal.

---

<sup>1</sup>e.g., 30X sequence coverage corresponds to 150X physical coverage.



## 1.1.3 Sequencing Signatures to Detect SVs

### 1.1.3.1 Read Pair

Read pair signatures can be used on Illumina sequencing data [33]. Normally we expect one end of the pair to map forward strand, other to reverse strand. However, on structural variation breakpoints this is not the case [7]. Variants and observed read pair signatures are shown in Table 1.1.3.1, where + denotes forward and – denotes the reverse strand.

Table 1.1: Read pair signatures and corresponding structural variants. for +- signature to be discordant, distance between read pairs should be larger than  $\mu + 3\sigma$ .

Mapping Strands	Variants
++	Inversions and Inverted Duplications
+-	Deletions, Interspersed Duplications and Translocations (Figure 4.2)
-+	Interspersed Duplications and Tandem Duplications
--	Inversions and Inverted Duplications

### 1.1.3.2 Split read

Split read based methods [3] aim to identify structural variations using reads that map to breakpoints of the events. Long read SV callers extensively use this signature. Since it shortens the sequence length further, this signal less suitable for short read technologies. However, they are useful to refine breakpoints of smaller events and it can provide additional support to read pair signatures.

### 1.1.3.3 Read depth

Read depth is a simple yet effective method for copy number variations. Whole genome is simply split into bins. For each read bin at the mapping location is

incremented. Some of the sequencing technologies suffer from GC bias, where regions with high G and C base density are less likely to be sequenced. This bias can be corrected statistically [34, 35]. If depth of a bin is smaller than expected range (can be  $\mu - 3\sigma$ ), it signals a deletion. If depth is larger than expected range ( $\mu + 3\sigma$ ), it signals a duplication. These bins can either be used to identify copy number variations, by checking the depth of bins at non-gap regions, or they can be used to support predictions made by other signatures (e.g., read pairs). If standard deviation of the depth values is high, it will be difficult to distinguish heterozygous variations from the normal. Also, in the complex regions of the genome, mapping ambiguity will render this SV signal less useful [13].

#### 1.1.4 Currently available structural variation discovery tools

##### 1.1.4.1 Short read based tools

First tool that was developed to discover SVs using HTS was PEMer [6]. It used Roche/454 sequencing, which is mostly abandoned today. The 1000 Genomes Project [32] raised interest on the SV discovery, predominantly for the Illumina platform. First read-pair based method for this platform was **VariationHunter** [36]. VariationHunter uses read pair signatures with read depth to identify deletions, inversions, transposon insertions and small novel sequence insertions. It clusters its predictions by approximating maximum set-cover problem. **Pindel** [37] is another method that uses paired short read data. Pindel looks for potential split reads and tries to map unmapped part of the read around its mate using pattern growth algorithm. **DELLY** [38] uses read pair signatures together with split read signatures to detect structural variations. It can call deletions, inversion and tandem duplications. It uses maximal cliques to cluster its predictions. Even though it has high recall rate in the simulations, it is imprecise for large SV detection. **LUMPY** [11] uses read pair signatures, read depth signatures and split read signatures together in a probabilistic framework to call structural variants. Although this tool makes precise predictions, it has

relatively low recall rate for large variants compared to other tools.

#### 1.1.4.2 Long read based tools

**SMRT-SV** [39] collects long reads that show split read signatures and constructs a *de novo* assembly. By remapping the assembled reads to the reference, it calls structural variants. **Sniffles** [16] is another SV discovery tool that utilizes long reads. Developers suggest using their own aligner, NGMLR, to map long reads. NGMLR uses a convex gap-cost scoring scheme, which is stated to be better suited for SV discovery with long reads. Together with improved split detection of NGMLR, Sniffles finds reads that indicate structural variants and cluster them. It can detect complex regions and partially phase the variants.

#### 1.1.4.3 Linked read based tools

**LongRanger** [30] is a comprehensive software package developed by 10x Genomics, for the purpose of barcode-aware read alignment and resolving full-scale human germline genome variation. **GROC-SV** is an optimized tool for somatic and complex SVs in cancer genomes. Both Long Ranger and GROC-SVs employ a novel idea to utilize discordance in expected “barcode coverage” as well as barcode similarities across distant locations for potential large-scale SV signals. In addition, GROC-SVs [31] performs local assembly on barcoded reads to detect large complex events that are between 10-100 Kbp with breakpoint resolution.

## Chapter 2

# VALOR<sub>2</sub> Algorithm to Discover Large SVs using Linked-Reads

### 2.1 Motivation

Structural variants that are within coding regions of the genome are associated with various syndromes [40, 34, 41, 42, 43]. Accurate detection of SVs can be beneficial to medical diagnosis and personalized treatments. Duplication of a 3.7 Mb segment at the 17p11.2 locus induces Potocki-Lupski Syndrome [44, 45]. Infants with this syndrome likely to show developmental delay, heart defects, dental and skeletal abnormalities. People with this syndrome show features of autism spectrum disorder, affecting social interaction and communication. Deletion of the same region causes Smith-Magenis syndrome [46]. Patients with this variation exhibit mild to moderate intellectual disability, delayed language skills, and behavioral problems. Inversions at 15q11-q13 locus causes Angelman Syndrome [42]. Patients with this syndrome shows delayed development, intellectual disability, severe speech impairment, and problems with movement and balance [47].

Accurate characterization of the structural variants can enhance our understanding of many genetic medical conditions. Furthermore, better annotation of SVs can benefit genome-wide association studies.

Even if structural variants do not intersect with any coding genes, they can alter 3D structure of chromosomes. 3D organization and folding of a chromosome can close up distances between positions that are distant on the linear sequence. Frequency of interactions between genetic sequences is dependent on the 3D positioning of those sequences. This correlation to proximity introduces Topologically Associating Domains (TADs). TADs are regions in the genome that host sequences with high levels of interaction with sequences within the same TAD and fewer interactions with others. Structural variants are shown to disrupt TAD's, thus change the 3D structure of the genome. Some of these disruptions to the genome structure shown to cause developmental disorders [48].

There are many algorithms to predict structural variants, yet for large variants (> 100Kb) they have poor precision and/or recall. Moreover, none of the available tools can call interspersed duplications (inverted or direct). Further details on the state-of-the-art algorithms are discussed in Section 1.1.4.

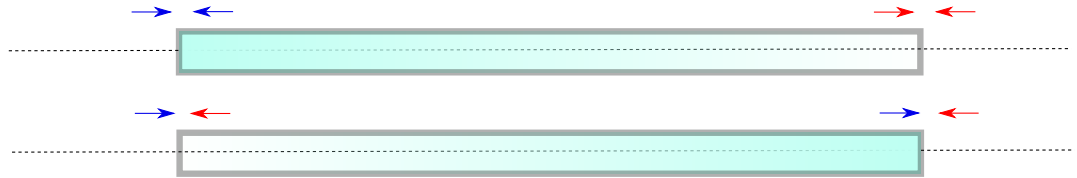
## 2.2 Challenge

Breakpoints of both inversions and segmental duplications lie on repeated regions [49] [50]. Because of this, mapping quality of reads around the breakpoints of these variants are reduced significantly and this makes it difficult to find these events with adequate accuracy. Recent developments with the long read technologies provided reads with sizes that can span repeated regions. However, high error rates makes it difficult to discover large variants with long reads alone.

Despite there have been studies on discovering existence of segmental duplications with read-depth based methods, pinpointing their insertion locus is a non-trivial task.

In a recent study, 54% of the previously predicted inversions reported by 1000GP shown to be inverted duplications [51, 32]. This is due to read-pair signatures (Figure 2.1) of inversions and inverted duplications being identical. While ordering of the pairs are different for these variants, in repeated regions (where these events likely to occur) mapping is not precise enough to differentiate them.

a)



b)

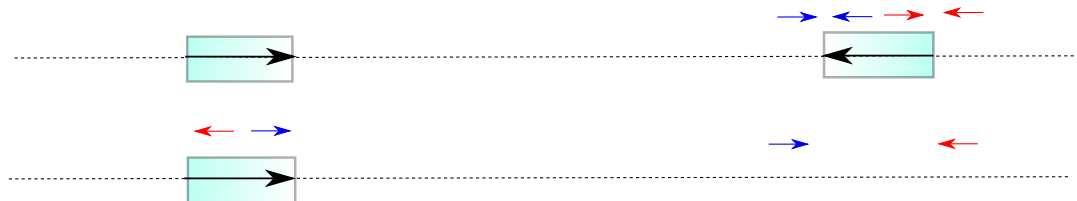


Figure 2.1: Read pair signatures for a) inversion, b) interspersed inverted duplication. Note that both variants show ++ and – read-pair signatures.

50% of genome consists of repeated sequences. Some of the reads in the repeated regions may align hundreds of positions with same alignment score, causing mapping ambiguity [14]. BWA-MEM [52] gets around this problem by randomly selecting one of the alignments and setting its score to zero. Firtina, *et al.* shows that many SV discovery tools fail to reproduce their results if input reads to aligner is shuffled [13].

## 2.3 Linked-Read data

This is a sequencing technique that uses micro-fluids to partition and barcode DNA fragments. This method provides long range information in addition to sequencing information. Large DNA fragments are separated into pools and bar-coded. Each pool contains up to 30 fragments and each molecule sequenced with very low coverage ( $\approx 0.2X$ ). Sequencing molecules with low coverage achieves high molecule coverage of the genome with relatively low cost, where 40X genome coverage with 0.2X molecule coverage achieves 200X physical coverage of genome with molecules.

## 2.4 Mapping linked-reads

VALOR<sub>2</sub> does not depend on any specific aligner for read mapping. In this study we used LongRanger aligner of 10x Genomics to map our simulated data. However, it is possible to preprocess reads to extract barcodes and align with any other aligner (e.g., BWA [52]).

## 2.5 Processing alignments

### 2.5.1 Determining read fragment size distribution parameters

For short reads, we expect fragment sizes to follow a Gaussian distribution. However, distribution mean and variation vary across samples. In order to reveal which range of fragment sizes are indeed concordant, we process a fixed number of reads (we use 1 million in this work) and calculate mean and standard deviation of the fragment size distribution of this sub-sample.

## 2.5.2 Loading and grouping reads

We separate reads into concordant and discordant read groups, where we define concordant reads to be  $+-$  aligned reads on the same chromosome with a size in the range of  $\mu \pm 3\sigma$ . Then, we classify discordant read pairs into eight groups (See Subsections 1.1.3.1 and 4.1.2). Four of the discordant types indicate intra-chromosomal variations (Table 1.1.3.1) and other four indicate interchromosomal variations (Table 4.1.2).

## 2.6 Recovering molecules

To recover 10xG molecules, we want to merge reads with the same barcode that are in close proximity with each other. VALOR<sub>2</sub> recovers 10xG molecules by merging concordant intervals with the same barcode that are in close proximity with each other. To do this efficiently, we stable sort concordantly mapped intervals that are already position sorted with respect to their barcode. Subsequently we can recover molecules with a single pass as shown in the Algorithm 1.



---

**Algorithm 1** Molecule recovery.

---

**Require:** Alignments in BAM format with barcodes, look-ahead parameter ( $Q$ ),  
extend parameter ( $T$ ).

**Ensure:** Set of submolecules  $S_M = \{M_1, M_2 \dots, M_k\}$  (value of  $k$  is unknown and  
will be determined by the algorithm)

$S_M \leftarrow \emptyset$

$i \leftarrow 1$

**for** each chromosome  $c$  **do**

**for** each barcode  $b$  **do**

$M_i = \emptyset$

**for**  $l = 1$  to  $\text{length}(c)$  **do**

**if** short fragment  $f$  with barcode  $b$  maps to  $c[l]$  **then**

**if**  $M_i = \emptyset$  **then**

$M_i \leftarrow f$

$s(M_i) \leftarrow s(f)$

$e(M_i) \leftarrow e(f)$

**else if** ( $s(f) < s(M_i) + Q$ ) **or** ( $s(f) < e(M_i) + T$ ) **then**

$M_i \leftarrow M_i \cup f$

$e(M_i) \leftarrow e(f)$

**else**

$S_M \leftarrow S_M \cup M_i$

$i \leftarrow i + 1$

**end if**

**end if**

**end for**

**end for**

**end for**

**return**  $S_M$

---

$s(f)$  denotes the map start location and  $e(f)$  denotes the map end location of  
fragment  $f$ .

---

## 2.6.1 Molecule depth signature

Read depth is a strong tool for detecting and verifying copy number variants [34, 35]. We introduce molecule depth signature, similar to barcode depth defined by GROC-SVs [31], while it has the filtering capabilities of read depth signature, it does not suffer from GC bias. We assume that, it follows Gaussian distribution (Figure 2.2), which allows us to make accurate filtering of copy number variation predictions.

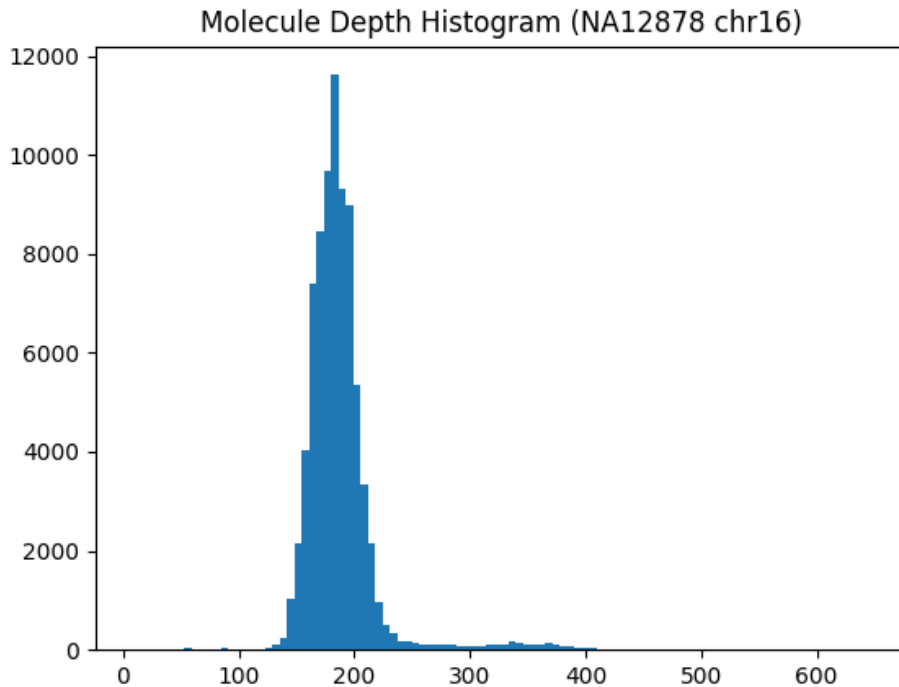


Figure 2.2: Molecule depth histogram of NA12878 in chr16 of non-zero bins. Data from [1, 2]

For each chromosome,  $\text{VALOR}_2$  allocates an integer array of  $\text{size}(\text{chr})/\text{bin\_size}$ . Then for each recovered molecule, respective bins from its start position to end position are incremented (Algorithm 2). To compute depth of the variations, it simply takes the average of the bins that intersect with the variation.

---

**Algorithm 2** Molecule Depth Computation

---

**Require:** Recovered 10xG Molecules, Number of base pairs in the chromosome ( $N$ ), Size of the depth bins ( $B$ ).

**Ensure:**  $A$  = Integer array of molecule depths with the size of  $N/B$

$A \leftarrow \text{Array}[N/B]$

**for**  $i = 0$  to  $N/B$  **do**

$A[i] \leftarrow 0$

**end for**

**for**  $m$  in Molecules **do**

**for**  $i = s(m)$  to  $e(m)$  increment by  $B$  **do**

$A[i/B] \leftarrow A[i/B] + 1$

**end for**

**end for**

**return**  $A$

---

$s(f)$  denotes the map start location and  $e(f)$  denotes the map end location of molecule  $m$ .

---

Molecules that map to gap and satellite regions introduce many false positive signals. We avoid erroneous predictions by removing molecules that overlap with those. Since molecules with a unique barcode cannot possibly be a split molecule, those are removed after read depths are computed.

## 2.7 Split molecule discovery

Although small set of molecules share same barcode (between 2 and 30 in 10xG data), two different molecules in the same chromosome can share a barcode. This makes split molecule discovery a nontrivial problem. We bypass this problem by generating all candidate split molecules and later filtering the ones with low discordant read support.

## 2.8 Matching split molecules

Split molecule signatures are simple and useful abstractions to define structural variation with Linked-Reads (Figure 2.3). Yet it is not as straightforward to spot these signatures from mapping information. It is not possible to figure out identities of the sub-molecules (A, B, C or D from Figure 2.3), before they are matched.

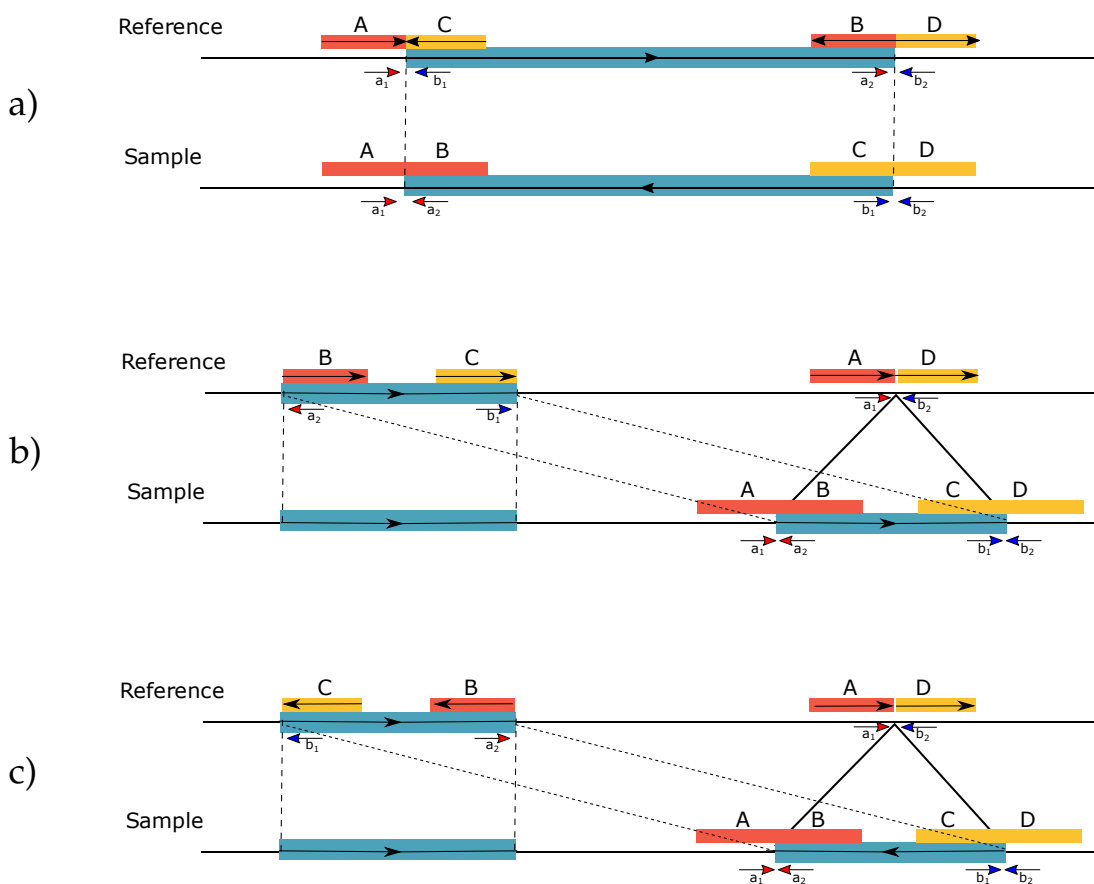


Figure 2.3: Split molecule and read pair sequence signatures used in VALOR<sub>2</sub>. a) Inversion, b) interspersed duplication in direct orientation, c) inverted duplication. In each case, the large molecules that span the SV breakpoints are split into two mapped regions. Note that, it is not possible to determine the mapped strand of the split molecules shown here. From the perspective of the reference genome (i.e., mapping), A,B,C,D are defined as *submolecules*, A/B and C/D pairs are *candidate splits*, and A/B-C/D quadruple is a *split molecule pair*.

Segmental duplications are asymmetric variations and their signature change with respect to relative position of the copy position (Figure 2.4). Furthermore, low coverage of the 10xG molecules makes it difficult to distinguish source and target of small duplications. We solve this problem by generating both possible scenarios and filtering them with read pair signatures (Algorithm 3).

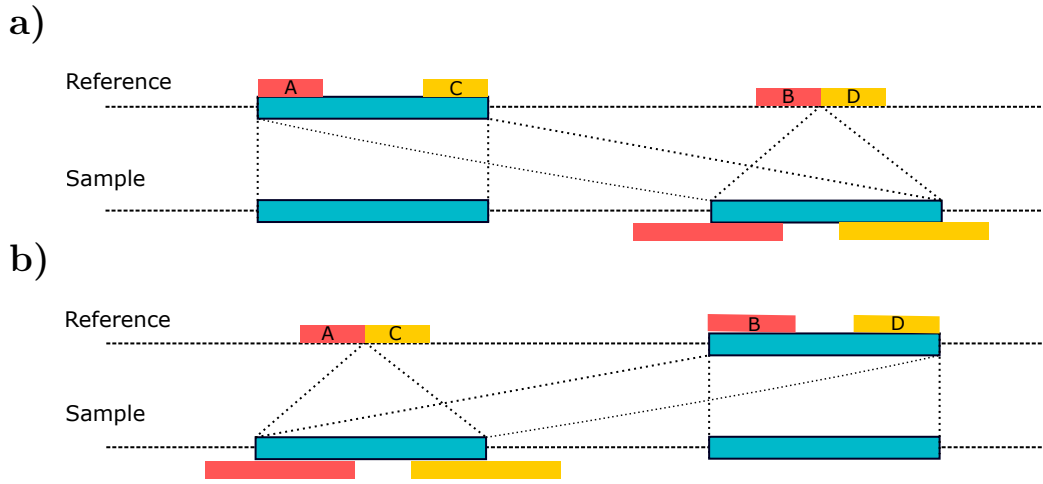


Figure 2.4: Asymmetric variations will have split molecule signatures for a) forward copy, b) backward copy direct interspersed duplications.

## 2.9 Filtering predictions with Illumina read pair signatures

For each split molecule of a SV candidate, read pair support values are calculated with the Algorithm 4. We remove candidates with any split molecules that are not supported. A higher threshold can be set according to coverage of the data.

## 2.10 Clustering predictions

High coverage of the HTS data allows us to build sensitive variant predictors. However, as a result of this many redundant calls indicating identical variants

---

**Algorithm 3** Split Molecule Matching

---

**Require:**  $S$  = Sorted array of split molecules,  $F$  is the list of variants VALOR<sub>2</sub> to discover.

**Ensure:**  $V$  = List of candidate variations

$V = \emptyset$

**for**  $s_{ab}$  in  $S$  **do**

**for**  $s_{cd} \neq s_{ab}$  in  $S$  **do**

**for**  $f$  in  $F$  **do**

**if**  $s_{ab}$  and  $s_{cd}$  indicates  $f$  **then**

$V \leftarrow V \cup f(s_{ab}, s_{cd})$

**end if**

**end for**

**end for**

**end for**

**return**  $V$

---

Two split molecules indicate a variant if they show signature of that variant together (Figure 2.3). VALOR<sub>2</sub> decides by comparing inner distance of the sub-molecules with predetermined gap and overlap constants and outer distance with predetermined minimum and maximum SV size constants.

---

will occur. To avoid reporting hundreds of identical calls we want to cluster our predictions and reduce overlapping variants into one.

Overlap between two structural variants is well defined. This allows us to use graph based clustering methods. Similar to the approach employed by Eslami-Rasekh *et al*, we decided to use quasi-clique approximation for variation clustering [29]. We added several optimizations specific to generated variant graph to the approximation algorithm to reduce running time.

### 2.10.1 Constructing SV graph

We construct a graph  $G(V,E)$  where  $V$  is the predicted variants and there are edges between 2 vertices if those variants overlap. Two variants overlap if, all of their split molecules overlap. Here we accept that two split molecules overlap if there is any intersection between their sub-molecules. This makes SV graph robust to partially recovered molecules due to low coverage and mapping ambiguity

---

**Algorithm 4** Read Pair Support Computation

---

**Require:**  $D$  = Sorted array of discordant reads of a type,  $s$  = A split molecule.

**Ensure:** Read pair support for  $s$  is updated

$mid \leftarrow DISCORDANT\_BINARY\_SEARCH(D, s)$

**for**  $j=mid$  to  $size(D)$  **do**

**if**  $D[j]$  overlaps with  $s$  **then**

$support(s) \leftarrow support(s) + 1$

**end if**

**if**  $e(s.A) < s(D[j].A)$  **then**

    Break

**end if**

**if**  $support(s) > MAX\_SUPPORT$  **then**

    ▷ Optional

    Break

**end if**

**end for**

---

$s(s)$  denotes the map start location and  $e(s)$  denotes the map end location of fragment  $f$ .

$s.A$  denotes the first fragment and  $s.B$  denotes the second fragment of split molecule or discordant read pair.

$DISCORDANT\_BINARY\_SEARCH(D, s)$  is a binary search function to find first discordant read pair that overlaps with a split molecule.

---

on repetitive regions. Furthermore this method accurately identifies predictions pointing to same variation, since it is unlikely to all four sub-molecules from different variations to intersect.

### 2.10.1.1 Patterns captured by SV graph

When we plot the SV graphs, we observe several patterns that can be used to identify some complex events such as; overlapping heterozygous variants, variants with single breakpoint on repeats and variants with both breakpoints on repeats (Figure 2.5).

## 2.10.2 Quasi-clique formulation to predict SVs

Ideally, SV graph will have a separate sub-graph for each structural variant. For repeat-free regions of the genome a simple DFS would be adequate to cluster structural variants. However, due to repetitiveness of the DNA there will be many outlier predictions in this graph. In this case if we use DFS to cluster variants, breakpoints will be skewed towards the outliers. In the other extreme if we use clique or an equivalent clustering technique, it will report completely connected components with low cardinality [29]. Thus this approach will report many equivalent clusters on the repeated regions. Maximal quasi-clique approximation [53] is able to cluster variants in the SV graph and it is robust to break-point ambiguities caused by repeated regions. VALOR<sub>2</sub> uses quasi-clique approximation together with the DFS to detect SV clusters (Algorithm 5).

---

**Algorithm 5** SV Clustering

---

**Require:**  $G(V, E) =$  Undirected SV graph.

**Ensure:**  $P =$  Clustered variations

$C \leftarrow \text{DFS\_FIND\_CONNECTED\_COMPONENTS}(G)$

**for**  $c$  in  $C$  **do**

$initial \leftarrow \text{size}(c)$

**while**  $initial * \alpha \leq \text{size}(c)$  **do**

$q \leftarrow \text{MAXIMAL\_QUASI\_CLIQUE}(c)$

$c \leftarrow c - q$

$P \leftarrow P \cup \text{RESOLVE\_SV\_BREAKPOINT}(q)$

**end while**

**end for**

**return**  $P$

---

$\alpha$  is a predetermined value between 0 and 1 to stop quasi-clique mining.  $\alpha$  can be set to 0 to find all clusters, 1 to find only 1 cluster,

$\text{size}(c)$  denotes the number of nodes in the subgraph  $c$

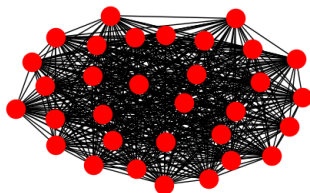
$\text{MAXIMAL\_QUASI\_CLIQUE}(c)$  is maximal quasi-clique approximation algorithm [53]

$\text{RESOLVE\_SV\_BREAKPOINT}(q)$  resolves breakpoints of clusters by averaging.

---



a)



b)



c)

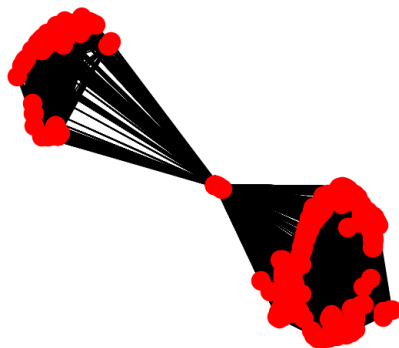


Figure 2.5: a) SV subgraph of a variant with low mapping ambiguity around the breakpoints. b) SV subgraph of a variant with breakpoints on highly repeated regions. c) SV subgraph of two heterozygous overlapping variants (from simulated data)

# Chapter 3

## Results

We tested VALOR<sub>2</sub> using both simulated and real data sets to compare the precision and recall rates of VALOR<sub>2</sub> with one other tool that use Linked-Read sequencing (Long Ranger [30], and two tools that use only Whole-genome shotgun (WGS) data sets (DELLY [38] and LUMPY [11]). However, VALOR<sub>2</sub> is the only tool that can characterize interspersed duplications, therefore we limit our comparison to only inversions, and evaluate VALOR<sub>2</sub>'s performance on duplications using simulations. We find that VALOR<sub>2</sub> is complementary to other methods in inversion calls as VALOR<sub>2</sub> aims to find larger (>80Kbp) inversions, while the other tools focus on smaller (<100 Kbp) SVs.

### 3.1 Simulated data

#### 3.1.1 Linked-Read simulation

We generated initial variation simulated represented as a VCF (Variation call format) file using VarSim [54]. VarSim does not generate any interspersed duplications by default. Therefore we randomly replaced some of the tandem duplication and insertion variants with interspersed duplications. Then we applied these

variants to a diploid genome and generated Linked-Reads using LRSIM [55].

### 3.1.2 Inserted variants

In this study we focused on discovery of inversions and interspersed duplications. However, to test the accuracy of VALOR<sub>2</sub> in the presence of other variants, we inserted 2,852,839 SNPs, 194,250 indels, 1,755 deletions, 2,225 insertions, 459 inversions, 584 tandem duplications and 260 interspersed duplications with sizes between 50 base pairs to 6 million base pairs (Table 3.1).

Table 3.1: Simulation statistics as generated by VarSim.

Variant type	Size range	# of variants
SNP	1 bp	2,852,839
Indel	1-50 bp	194,250
Deletion	50 bp - 6 Mbp	1,755
Insertion	50 bp - 6 Mbp	2,245
Inversion	50 bp - 6 Mbp	459
Tandem duplication	50 bp - 6 Mbp	584
Interspersed duplication	50 bp - 6 Mbp	260 (110 inverted, 150 direct)

### 3.1.3 Simulated results and comparison with other methods

We present the prediction performance of the tools we tested in Table 3.2. We found that VALOR<sub>2</sub> is able to correctly predict >82% of large duplications (inverted and direct combined), and 76% of large inversions, while maintaining 92–96% precision for duplications and 98% precision for inversions. Long Ranger, the other algorithm that used Linked-Reads, correctly predicted 72% of the inversions with 71% precision. Of the WGS-based tools, DELLY achieved high sensitivity for inversions and it was able to correctly predict 84% of large inversions, however it suffered from very low precision (15%). On the contrary,

Table 3.2: Prediction performance evaluation using simulated structural variants.

Variant	Tool	# Sim	# Calls	Precision	Recall
Duplication (direct)	VALOR <sub>2</sub>	78	66	0.92	0.78
Duplication (inverted)	VALOR <sub>2</sub>	56	51	0.96	0.88
Inversion	VALOR <sub>2</sub>	94	65	0.98	0.76
	LUMPY		42	0.90	0.47
	DELLY		896	0.15	0.84
	Long Ranger		92	0.71	0.72

We evaluate prediction performance of only large (>80Kbp for inversions, >40Kbp for duplications) SVs. Note that LUMPY, DELLY, and Long Ranger are not able to call interspersed duplications, thus we provide only the inversion prediction benchmark. Precision is calculated as  $\frac{TP}{TP+FP}$ , and recall is defined as  $\frac{TP}{TP+FN}$ , where TP: true positive, FP: false positive, FN: false negative.

LUMPY achieved high precision (90%), but it was able to discover only 47% of the simulated inversions. This is likely because neither DELLY nor LUMPY were optimized to find such large inversion events. Overall, VALOR<sub>2</sub> performed the best in terms of precision and recall balance in the simulation experiment.

## 3.2 Real data

### 3.2.1 NA12878

We also compared the performance of VALOR<sub>2</sub> with that of Long Ranger on the NA12878 germline genome, along with other commonly used SV callers (DELLY and LUMPY). NA12878 variant calls were obtained from 10X Genomics on their Chromium platform. From these we extracted 476 large inversions, 14 of which were also present in the InvFEST database (Table 3.3) but only one was experimentally validated. When given the same data, VALOR<sub>2</sub> was able to call 135 inversions, a higher percentage of which were found in the InvFEST database that also included six experimentally validated inversions. Of the four tools we tested, VALOR<sub>2</sub> had the largest number of validated inversions within its call set while predicting the second lowest number of total inversions (only LUMPY,

which only called 7 inversions, has fewer). This result further highlights the superior precision and recall of VALOR<sub>2</sub>. DELLY was able to identify 24 inversions in the NA12878 genome which were also in the InvFEST database but called a total of 2,340 inversions. A majority of these calls were only predicted by DELLY and due to a lack of precision, may signify an over-representation of false positives (Figure 3.1). VALOR<sub>2</sub> was very useful in identifying large scale duplications by exploiting linked read information in the NA12878 sequencing data. We predicted multiple direct segmental duplications and inverted duplications with chromosomes 1 and 16 containing both classes of duplications (Table 3.4).

Table 3.3: Inversion prediction performance evaluation in the NA12878 genome using InvFEST database.

	Called	InvFEST-Valid.	InvFEST-Pred.	InvFEST-All
VALOR <sub>2</sub>	135	6	5	17
Long Ranger	476	1	10	14
LUMPY	7	0	0	0
DELLY	2,340	1	6	24

Here we only focus on large (> 80Kbp) inversions in the NA12878 genome. InvFEST-Valid.: validated inversions in the genome of NA12878, InvFEST-Pred.: predicted inversions in the genome of NA12878, InvFEST-All: all inversions reported in the InvFEST database [56], except those that are annotated as *unreliable prediction*.

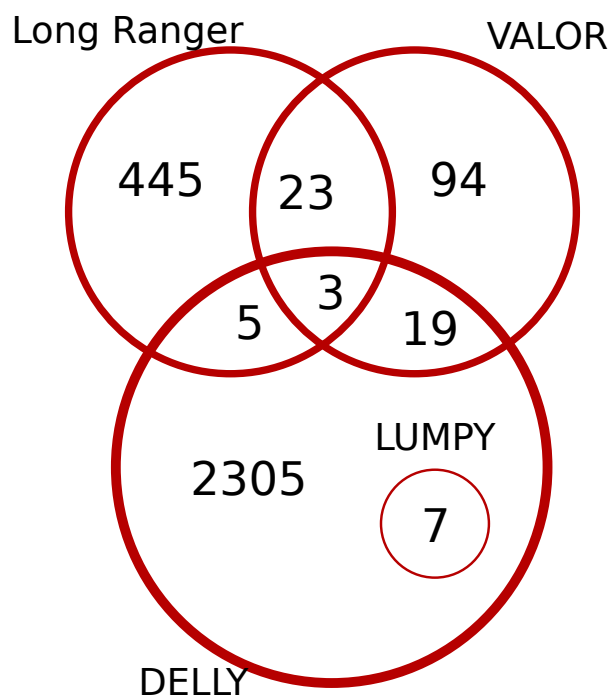


Figure 3.1: Comparison of the inversion predictions (> 80 Kb) by VALOR<sub>2</sub>, Long Ranger, DELLY, and LUMPY in the NA12878 genome.

### 3.2.2 CHM1

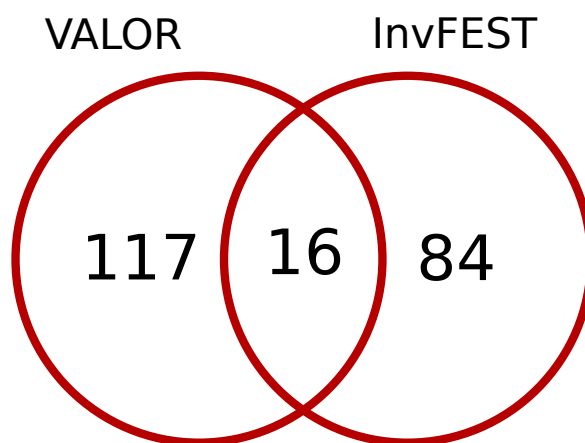


Figure 3.2: Intersection of all inversions reported by InvFEST (validated or predicted) with VALOR<sub>2</sub> predictions on CHM1 genome.

Table 3.4: Segmental duplications predicted in the NA12878 genome using VALOR<sub>2</sub>.

Chr	Start	End	Type	Target	No. of genes
1	120,600,786	120,692,870	Direct	1q21.1	1
1	144,832,884	145,751,706	Direct	1p22.3	25
1	145,062,336	145,116,024	Direct	1p11.2	
16	86,451,165	86,498,200	Direct	16q11.2	
17	21,522,544	21,551,840	Direct	17p11.2	
1	17,019,657	17,111,181	Inverted	1q42.3	4
1	145,983,326	146,027,347	Inverted	1p22.3	3
4	15,160	67,199	Inverted	4q35.2	2
8	2,189,297	2,290,508	Inverted	8p23.2	
10	46,965,140	47,022,150	Inverted	10q11.22	2
11	4,250,956	4,331,367	Inverted	11p15.4	
16	21,542,145	21,593,639	Inverted	16p12.2	
16	22,543,245	22,709,969	Inverted	16p12.2	2
X	153,423,995	153,485,001	Inverted	Xq28	3

We tested VALOR<sub>2</sub> using Linked-Read data set of a haploid human genome cell line (CHM1 [57, 58, 59]). We used VALOR<sub>2</sub> to find inversions and segmental duplications. Overall, VALOR<sub>2</sub> characterized 133 inversions (>80 Kbp), 14 inverted and 22 direct segmental duplications (>40 Kb). Unfortunately there are no gold standard data sets for segmental duplications for this genome available in the literature, and the largest previously reported inversion in [59] is 36 Kbp, which is less than the smallest inversion that VALOR<sub>2</sub> predicts. We therefore compared only with the large inversions in the InvFEST database, and we found that 10% (16/117) of VALOR<sub>2</sub> predictions were present in InvFEST (Figure 3.2).

# Chapter 4

## Discussion and Future Work

In this thesis, we present novel algorithms to effectively utilize the encoded long-range information in Linked-Read data for the purpose of characterizing large-scale structural variations. The current state-of-the-art SV detection techniques using Linked-Read like Long Ranger are optimized for certain range of SV sizes. However, VALOR<sub>2</sub> can detect events including segmental duplications of sizes larger than 100 Kb with high precision.

Downside of the VALOR<sub>2</sub> algorithm is that, minimum size of its predictions is limited by molecule size of the sequencing platform. Furthermore, due to low coverage of the molecules and miss-mappings, it is difficult to assess sizes of the molecules from mapping positions. Another issue that needs improvement in VALOR<sub>2</sub> algorithm is low specificity at smaller events.

In general VALOR<sub>2</sub> offers precise predictions for large structural variations. It is robust to mapping ambiguity and there is no theoretical upper bound for the sizes it can discover. It is designed to be complementary to the SV detection algorithms that target smaller variants.



## 4.1 Works in progress

### 4.1.1 Deletion discovery

In addition to inversions and segmental duplications, we also implemented a prototype algorithm for deletion discovery in VALOR<sub>2</sub>. Unlike other intra-chromosomal variations, deletions show single split molecule and read-pair signatures (Figure 4.1). To further improve accuracy of VALOR<sub>2</sub> we apply molecule depth filtering and remove predictions with depth  $> \mu/2 + \sigma$  (Figure 2.2).

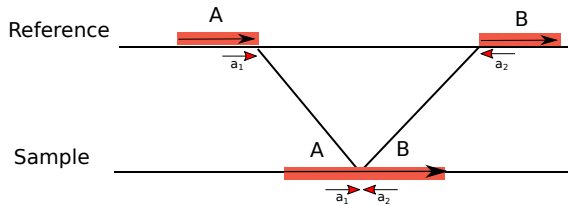


Figure 4.1: Split molecule and read pair signature of a deletion.

While in the preliminary simulation results VALOR<sub>2</sub> was the most precise, its recall was lower than other tools (Table 4.1). We’re currently investigating the causes for the low recall rate and cases where VALOR<sub>2</sub> overlooks deletions.

Table 4.1: Prediction performance evaluation using simulated deletions.

Variant	Tool	# Simulated	# Predicted	Precision	Recall
Deletion	VALOR <sub>2</sub>	71	54	0.98	0.76
	LUMPY		264	0.22	0.83
	DELLY		640	0.11	0.89
	Long Ranger		168	0.42	0.93

We evaluate prediction performance of only large ( $>90\text{Kbp}$ ) deletions. Precision is calculated as  $\frac{TP}{TP+FP}$ , and recall is defined as  $\frac{TP}{TP+FN}$ , where TP: true positive, FP: false positive, FN: false negative.

### 4.1.2 Inter-chromosomal events

In 10xG Linked-Read data a barcode may be seen in up to 30 different molecules randomly distributed to whole genome. In a single chromosome this corresponds to 2 ~ 5 molecules. VALOR<sub>2</sub> exploits the fact that number of false candidate splits is between  $\binom{5}{2} = 10$  where there are no splits in any of molecules with that barcode and  $\binom{5*2}{2} = 45$  where all molecules of that barcode are split. Even in the worst case, complexity introduced by exhaustive split checking is negligible for intra-chromosomal variations. Also you should note that reaching the upper bound of this range is quite unlikely.

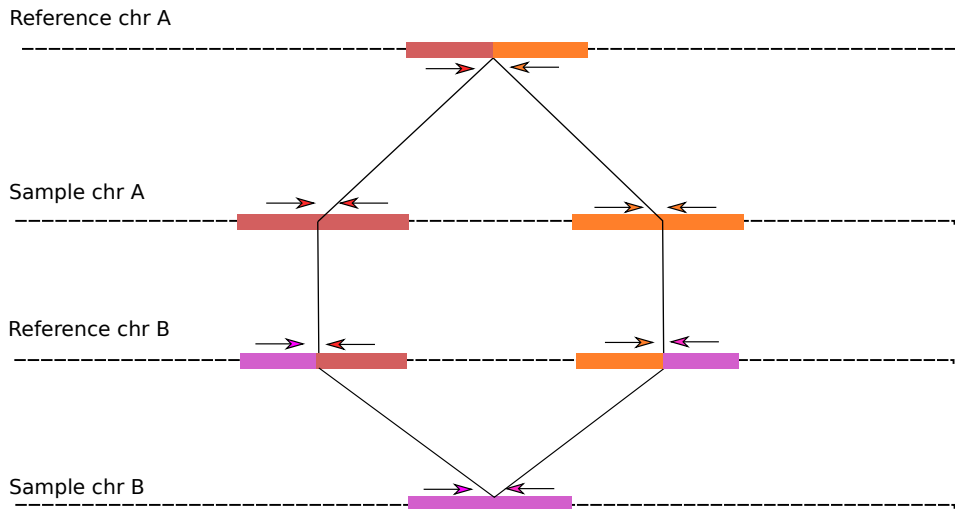


Figure 4.2: Split molecule and read pair signature of translocation. Where a segment of DNA is copied from chromosome B to A.

Yet, exhaustive trial of split molecules is infeasible for inter-chromosomal events. Since expected number of molecules for each barcode is ~30, for each barcode we are required to check hundreds to thousands of false split candidates. Moreover, split molecule signature of translocations involve 3 splits (Figure 4.2), which further increases the complexity.

Table 4.2: Read pair signatures and corresponding interchromosomal structural variants. Each pair should map to different chromosomes

Mapping Strands	Variants
++	Inverted Translocations and Inverted Duplications
+-	Direct Duplications and Direct Translocations
-+	Direct Duplications and Direct Translocations
--	Inverted Translocations and Inverted Duplications

To resolve this problem, we designed a complementary algorithm to VALOR<sub>2</sub> for inter-chromosomal events. For each barcoded read pair with ends on different chromosomes, we search for molecules of the same barcode near each read (Figure 4.3). Since coverage of each molecule is low, only a few of the molecules will contain a discordant read and majority of the split molecules will be overlooked. But we can recover rest of the split molecules by searching molecules around the initially discovered splits. Rest of the algorithm is very similar to original VALOR<sub>2</sub>, where algorithm is executed for each chromosome pair instead of each chromosome.

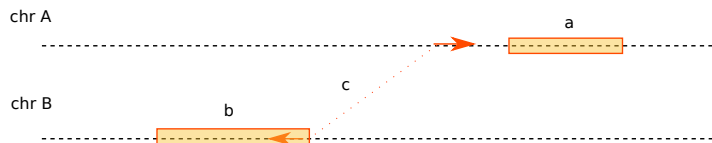


Figure 4.3: a and b are molecules with the same barcode in different chromosomes. c is a discordant read pair with one end near a other end near b. We allow gaps between reads and molecules to cover for low coverage. We allow overlaps to be robust to repeats.

## 4.2 Future directions

### 4.2.1 Structural variation discovery on tumor samples

Due to their uncontrolled division, tumor cells mutate frequently. Consequently many structural variations which cannot be observed on germline samples can be found at tumor cells. However, structural variation discovery on somatic samples is not a straight-forward task. Heterogeneous nature of somatic samples makes it difficult predict variations, since coverage of the variants change in proportion to their frequency in the sample cells. Yet, discovery of structural variation on tumor samples is worth exploring as it can enhance our understanding of cancer.

### 4.2.2 Resolving overlapping events

In a recent study 21% of the previous inversion predictions shown to contain one or more deletions [51]. Overlapping variations are rare on a germline sample of a healthy human (compared to human genome reference). Yet studies on multiple species, ancient humans and cancer can benefit from accurate characterization of overlapping structural variation. While some of the overlapping variations can hide split molecule signatures, VALOR<sub>2</sub> can be modified to identify overlapping variants with visible signatures.

### 4.2.3 Expanding the range of predictions

Because of the low coverage of 10xG molecules, it is difficult to detect short-range splits. For this reason, we limited VALOR<sub>2</sub> to only discover inversions and deletions with size  $> 2\mu$  and duplications with size  $> \mu$ , where  $\mu$  is the mean molecule size. Inversion and deletion splits map around variant breakpoints, on the other hand duplication splits map to source and copy positions. Hence, vagueness of small splits influence minimum copy distance, rather than duplication size. Yet we

choose to limit minimum duplication size to ensure that  $\text{VALOR}_2$  can confidently recover split molecules. While it is not feasible to reduce this limit for inversions and deletions, it is doable for duplications. We can expand split molecule model to allow barcoded discordant reads to form split molecules with other molecules with the same barcode (Figure 4.4).

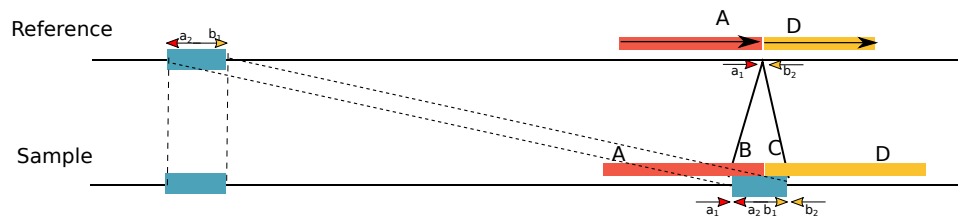


Figure 4.4: A model to discover smaller duplications, where split molecule information is lost due to small size of the duplication. We can look for discordant read pairs which share barcodes with the molecules around the target. AB and CD molecules are on the duplication, B and C are lost due to low coverage.

# Bibliography

- [1] J. M. Zook, B. Chapman, J. Wang, D. Mittelman, O. Hofmann, W. Hide, and M. Salit, “Integrating human sequence data sets provides a resource of benchmark snp and indel genotype calls,” *Nat Biotechnol*, vol. 32, pp. 246–251, Mar 2014.
- [2] J. M. Zook, D. Catoe, J. McDaniel, L. Vang, N. Spies, A. Sidow, Z. Weng, Y. Liu, C. E. Mason, N. Alexander, E. Henaff, A. B. R. McIntyre, D. Chandramohan, F. Chen, E. Jaeger, A. Moshrefi, K. Pham, W. Stedman, T. Liang, M. Saghbini, Z. Dzakula, A. Hastie, H. Cao, G. Deikus, E. Schadt, R. Sebra, A. Bashir, R. M. Truty, C. C. Chang, N. Gulbahce, K. Zhao, S. Ghosh, F. Hyland, Y. Fu, M. Chaisson, C. Xiao, J. Trow, S. T. Sherry, A. W. Zaranek, M. Ball, J. Bobe, P. Estep, G. M. Church, P. Marks, S. Kyriazopoulou-Panagiotopoulou, G. X. Y. Zheng, M. Schnall-Levin, H. S. Ordonez, P. A. Mudivarti, K. Giorda, Y. Sheng, K. B. Rypdal, and M. Salit, “Extensive sequencing of seven human genomes to characterize benchmark reference materials,” *Scientific data*, vol. 3, p. 160025, June 2016.
- [3] C. Alkan, B. P. Coe, and E. E. Eichler, “Genome structural variation discovery and genotyping,” *Nat Rev Genet*, vol. 12, pp. 363–376, May 2011.
- [4] F. Sanger and A. Coulson, “A rapid method for determining sequences in dna by primed synthesis with dna polymerase,” *Journal of Molecular Biology*, vol. 94, no. 3, pp. 441 – 448, 1975.
- [5] “Summary of findings – cost-effectiveness of next generation sequencing,” Feb 2014.

- [6] J. O. Korbelt, A. E. Urban, J. P. Affourtit, B. Godwin, F. Grubert, J. F. Simons, P. M. Kim, D. Palejev, N. J. Carrero, L. Du, B. E. Taillon, Z. Chen, A. Tanzer, A. C. E. Saunders, J. Chi, F. Yang, N. P. Carter, M. E. Hurles, S. M. Weissman, T. T. Harkins, M. B. Gerstein, M. Egholm, and M. Snyder, "Paired-end mapping reveals extensive structural variation in the human genome," *Science*, vol. 318, pp. 420–426, Oct 2007.
- [7] F. Hormozdiari, C. Alkan, E. E. Eichler, and S. C. Sahinalp, "Combinatorial algorithms for structural variation detection in high-throughput sequenced genomes," *Genome Res*, vol. 19, pp. 1270–1278, Jul 2009.
- [8] P. Medvedev, M. Stanciu, and M. Brudno, "Computational methods for discovering structural variation with next-generation sequencing," *Nat Methods*, vol. 6, pp. S13–S20, Nov 2009.
- [9] S. Sindi, E. Helman, A. Bashir, and B. J. Raphael, "A geometric approach for classification and comparison of structural variants," *Bioinformatics*, vol. 25, pp. i222–i230, June 2009.
- [10] I. Hajirasouliha, F. Hormozdiari, C. Alkan, J. M. Kidd, I. Birol, E. E. Eichler, and S. C. Sahinalp, "Detection and characterization of novel sequence insertions using paired-end next-generation sequencing," *Bioinformatics*, vol. 26, pp. 1277–1283, May 2010.
- [11] R. M. Layer, C. Chiang, A. R. Quinlan, and I. M. Hall, "LUMPY: a probabilistic framework for structural variant discovery," *Genome Biol*, vol. 15, no. 6, p. R84, 2014.
- [12] A. Soylev, C. Kockan, F. Hormozdiari, and C. Alkan, "Toolkit for automated and rapid discovery of structural variants," *Methods*, vol. 129, pp. 3–7, 2017.
- [13] C. Firtina and C. Alkan, "On genomic repeats and reproducibility," *Bioinformatics*, vol. 32, pp. 2243–2247, Aug 2016.
- [14] T. J. Treangen and S. L. Salzberg, "Repetitive DNA and next-generation sequencing: computational challenges and solutions," *Nat Rev Genet*, vol. 13, pp. 36–46, Jan 2012.

- [15] A. C. English, W. J. Salerno, and J. G. Reid, “PBHoney: identifying genomic variants via long-read discordance and interrupted mapping,” *BMC Bioinformatics*, vol. 15, p. 180, 2014.
- [16] F. J. Sedlazeck, P. Rescheneder, M. Smolka, H. Fang, M. Nattestad, A. von Haeseler, and M. C. Schatz, “Accurate detection of complex structural variations using single-molecule sequencing.,” *Nature methods*, vol. 15, pp. 461–468, June 2018.
- [17] M. Jain, S. Koren, K. H. Miga, J. Quick, A. C. Rand, T. A. Sasani, J. R. Tyson, A. D. Beggs, A. T. Dilthey, I. T. Fiddes, S. Malla, H. Marriott, T. Nieto, J. O’Grady, H. E. Olsen, B. S. Pedersen, A. Rhie, H. Richardson, A. R. Quinlan, T. P. Snutch, L. Tee, B. Paten, A. M. Phillippy, J. T. Simpson, N. J. Loman, and M. Loose, “Nanopore sequencing and assembly of a human genome with ultra-long reads.,” *Nature biotechnology*, vol. 36, pp. 338–345, Apr. 2018.
- [18] A. Ritz, A. Bashir, S. Sindi, D. Hsu, I. Hajirasouliha, and B. J. Raphael, “Characterization of structural variants with single molecule and hybrid sequencing approaches,” *Bioinformatics*, vol. 30, pp. 3458–3466, Dec 2014.
- [19] Y. Mostovoy, M. Levy-Sakin, J. Lam, E. T. Lam, A. R. Hastie, P. Marks, J. Lee, C. Chu, C. Lin, . Džakula, H. Cao, S. A. Schlebusch, K. Giorda, M. Schnall-Levin, J. D. Wall, and P.-Y. Kwok, “A hybrid approach for de novo human genome sequence assembly and phasing.,” *Nature methods*, vol. 13, pp. 587–590, July 2016.
- [20] L. C. Xia, J. M. Bell, C. Wood-Bouwens, J. J. Chen, N. R. Zhang, and H. P. Ji, “Identification of large rearrangements in cancer genomes with barcode linked reads.,” *Nucleic acids research*, Nov. 2017.
- [21] S. Yeo, L. Coombe, R. L. Warren, J. Chu, and I. Birol, “ARCS: scaffolding genome drafts with linked reads.,” *Bioinformatics*, vol. 34, pp. 725–731, Mar. 2018.
- [22] J.-S. Seo, A. Rhie, J. Kim, S. Lee, M.-H. Sohn, C.-U. Kim, A. Hastie, H. Cao, J.-Y. Yun, J. Kim, J. Kuk, G. H. Park, J. Kim, H. Ryu, J. Kim, M. Roh,



- J. Baek, M. W. Hunkapiller, J. Korlach, J.-Y. Shin, and C. Kim, “De novo assembly and phasing of a Korean human genome.,” *Nature*, vol. 538, pp. 243–247, Oct. 2016.
- [23] N. I. Weisenfeld, V. Kumar, P. Shah, D. M. Church, and D. B. Jaffe, “Direct determination of diploid genome sequences.,” *Genome research*, vol. 27, pp. 757–767, May 2017.
- [24] D. C. Danko, D. Meleshko, D. Bezdan, C. Mason, and I. Hajirasouliha, “Minerva: an alignment and reference free approach to deconvolve linked-reads for metagenomics,” *bioRxiv*, 2017.
- [25] D. A. Skelly, G. T. Squiers, M. A. McLellan, M. T. Bolisetty, P. Robson, N. A. Rosenthal, and A. R. Pinto, “Single-cell transcriptional profiling reveals cellular diversity and intercommunication in the mouse heart.,” *Cell reports*, vol. 22, pp. 600–610, Jan. 2018.
- [26] F. A. Wolf, P. Angerer, and F. J. Theis, “SCANPY: large-scale single-cell gene expression data analysis.,” *Genome biology*, vol. 19, p. 15, Feb. 2018.
- [27] S. Aibar, C. B. González-Blas, T. Moerman, V. A. Huynh-Thu, H. Imrichova, G. Hulselmans, F. Rambow, J.-C. Marine, P. Geurts, J. Aerts, J. van den Oord, Z. K. Atak, J. Wouters, and S. Aerts, “SCENIC: single-cell regulatory network inference and clustering.,” *Nature methods*, vol. 14, pp. 1083–1086, Nov. 2017.
- [28] G. X. Y. Zheng, B. T. Lau, M. Schnall-Levin, M. Jarosz, J. M. Bell, C. M. Hindson, S. Kyriazopoulou-Panagiotopoulou, D. A. Masquelier, L. Merrill, J. M. Terry, P. A. Mudivarti, P. W. Wyatt, R. Bharadwaj, A. J. Makarewicz, Y. Li, P. Belgrader, A. D. Price, A. J. Lowe, P. Marks, G. M. Vurens, P. Hardenbol, L. Montesclaros, M. Luo, L. Greenfield, A. Wong, D. E. Birch, S. W. Short, K. P. Bjornson, P. Patel, E. S. Hopmans, C. Wood, S. Kaur, G. K. Lockwood, D. Stafford, J. P. Delaney, I. Wu, H. S. Ordonez, S. M. Grimes, S. Greer, J. Y. Lee, K. Belhocine, K. M. Giorda, W. H. Heaton, G. P. McDermott, Z. W. Bent, F. Meschi, N. O. Kondov, R. Wilson, J. A. Bernate, S. Gauby, A. Kindwall, C. Bermejo, A. N. Fehr, A. Chan,

- S. Saxonov, K. D. Ness, B. J. Hindson, and H. P. Ji, “Haplotyping germline and cancer genomes with high-throughput linked-read sequencing.,” *Nature biotechnology*, vol. 34, pp. 303–311, Mar. 2016.
- [29] M. Eslami Rasekh, G. Chiatante, M. Miroballo, J. Tang, M. Ventura, C. T. Amemiya, E. E. Eichler, F. Antonacci, and C. Alkan, “Discovery of large genomic inversions using long range information,” *BMC Genomics*, vol. 18, p. 65, Jan. 2017.
- [30] P. Marks, S. Garcia, A. M. Barrio, K. Belhocine, J. Bernate, R. Bhargava, K. Bjornson, C. Catalanotti, J. Delaney, A. Fehr, *et al.*, “Resolving the full spectrum of human genome variation using linked-reads,” *BioRxiv*, p. 230946, 2017.
- [31] N. Spies, Z. Weng, A. Bishara, J. McDaniel, D. Catoe, J. M. Zook, M. Salit, R. B. West, S. Batzoglou, and A. Sidow, “Genome-wide reconstruction of complex structural variants using read clouds.,” *Nature methods*, vol. 14, pp. 915–920, Sept. 2017.
- [32] The 1000 Genomes Project Consortium, “A map of human genome variation from population-scale sequencing,” *Nature*, vol. 467, pp. 1061–1073, Oct 2010.
- [33] E. Tuzun, A. J. Sharp, J. A. Bailey, R. Kaul, V. A. Morrison, L. M. Pertz, E. Haugen, H. Hayden, D. Albertson, D. Pinkel, M. V. Olson, and E. E. Eichler, “Fine-scale structural variation of the human genome,” *Nat Genet*, vol. 37, pp. 727–732, Jul 2005.
- [34] C. Alkan, J. M. Kidd, T. Marques-Bonet, G. Aksay, F. Antonacci, F. Hormozdiari, J. O. Kitzman, C. Baker, M. Malig, O. Mutlu, S. C. Sahinalp, R. A. Gibbs, and E. E. Eichler, “Personalized copy number and segmental duplication maps using next-generation sequencing,” *Nat Genet*, vol. 41, pp. 1061–1067, Oct 2009.
- [35] A. Abyzov, A. E. Urban, M. Snyder, and M. Gerstein, “CNVnator: an approach to discover, genotype, and characterize typical and atypical CNVs

- from family and population genome sequencing,” *Genome Res*, vol. 21, pp. 974–984, Jun 2011.
- [36] F. Hormozdiari, I. Hajirasouliha, P. Dao, F. Hach, D. Yorukoglu, C. Alkan, E. E. Eichler, and S. C. Sahinalp, “Next-generation VariationHunter: combinatorial algorithms for transposon insertion discovery,” *Bioinformatics*, vol. 26, pp. i350–i357, Jun 2010.
- [37] K. Ye, M. H. Schulz, Q. Long, R. Apweiler, and Z. Ning, “Pindel: a pattern growth approach to detect break points of large deletions and medium sized insertions from paired-end short reads,” *Bioinformatics*, vol. 25, pp. 2865–2871, Nov 2009.
- [38] T. Rausch, T. Zichner, A. Schlattl, A. M. Stütz, V. Benes, and J. O. Korbel, “DELLY: structural variant discovery by integrated paired-end and split-read analysis,” *Bioinformatics*, vol. 28, pp. i333–i339, Sep 2012.
- [39] J. Huddleston, M. J. Chaisson, K. Meltz Steinberg, W. Warren, K. Hoekzema, D. S. Gordon, T. A. Graves-Lindsay, K. M. Munson, Z. N. Kronenberg, L. Vives, P. Peluso, M. Boitano, C.-S. Chin, J. Korf, R. K. Wilson, and E. E. Eichler, “Discovery and genotyping of structural variation from long-read haploid genome sequence data,” *Genome research*, Nov. 2016.
- [40] H. C. Mefford and E. E. Eichler, “Duplication hotspots, rare genomic disorders, and common disease,” *Current opinion in genetics & development*, vol. 19, no. 3, pp. 196–204, 2009.
- [41] L. R. Osborne, M. Li, B. Pober, D. Chitayat, J. Bodurtha, A. Mandel, T. Costa, T. Grebe, S. Cox, L. C. Tsui, and S. W. Scherer, “A 1.5 million-base pair inversion polymorphism in families with Williams-Beuren syndrome,” *Nat Genet*, vol. 29, pp. 321–325, Nov 2001.
- [42] G. Gimelli, M. A. Pujana, M. G. Patricelli, S. Russo, D. Giardino, L. Larizza, J. Cheung, L. Armengol, A. Schinzel, X. Estivill, and O. Zuffardi, “Genomic

- inversions of human chromosome 15q11-q13 in mothers of Angelman syndrome patients with class ii (bp2/3) deletions,” *Hum Mol Genet*, vol. 12, pp. 849–858, Apr 2003.
- [43] R. Visser, O. Shimokawa, N. Harada, N. Niikawa, and N. Matsumoto, “Non-hotspot-related breakpoints of common deletions in sotos syndrome are located within destabilised dna regions,” *J Med Genet*, vol. 42, p. e66, Nov 2005.
- [44] L. Potocki, W. Bi, D. Treadwell-Deering, C. M. Carvalho, A. Eifert, E. M. Friedman, D. Glaze, K. Krull, J. A. Lee, R. A. Lewis, R. Mendoza-Londono, P. Robbins-Furman, C. Shaw, X. Shi, G. Weissenberger, M. Withers, S. A. Yatsenko, E. H. Zackai, P. Stankiewicz, and J. R. Lupski, “Characterization of potocki-lupski syndrome (dup(17)(p11.2p11.2)) and delineation of a dosage-sensitive critical interval that can convey an autism phenotype,” *The American Journal of Human Genetics*, vol. 80, no. 4, pp. 633 – 649, 2007.
- [45] C. R. Soler-Alfonso, K. J. Motil, C. L. Turk, P. J. Robbins-Furman, E. M. Friedman, F. Zhang, J. R. Lupski, J. K. Fraley, and L. Potocki, “Potocki-lupski syndrome: a microduplication syndrome associated with oropharyngeal dysphagia and failure to thrive.,” *The Journal of pediatrics*, vol. 158 4, pp. 655–659.e2, 2011.
- [46] P. Carmona-Mora, C. A. Encina, C. P. Canales, L. Cao, J. Molina, P. Kairath, J. I. Young, and K. Walz, “Functional and cellular characterization of human retinoic acid induced 1 (rail) mutations associated with smith-magenis syndrome,” *BMC Molecular Biology*, vol. 11, p. 63, Aug 2010.
- [47] K. Buiting, “Prader–willi syndrome and angelman syndrome,” *American Journal of Medical Genetics Part C: Seminars in Medical Genetics*, vol. 154C, no. 3, pp. 365–376.
- [48] L. Huynh and F. Hormozdiari, “Contribution of structural variation to genome structure: Tad fusion discovery and ranking,” *bioRxiv*, 2018.
- [49] J. M. Kidd, G. M. Cooper, W. F. Donahue, H. S. Hayden, N. Sampas, T. Graves, N. Hansen, B. Teague, C. Alkan, F. Antonacci, E. Haugen,

- T. Zerr, N. A. Yamada, P. Tsang, T. L. Newman, E. Tüzün, Z. Cheng, H. M. Ebling, N. Tusneem, R. David, W. Gillett, K. A. Phelps, M. Weaver, D. Saranga, A. Brand, W. Tao, E. Gustafson, K. McKernan, L. Chen, M. Malign, J. D. Smith, J. M. Korn, S. A. McCarroll, D. A. Altshuler, D. A. Peiffer, M. Dorschner, J. Stamatoyannopoulos, D. Schwartz, D. A. Nickerson, J. C. Mullikin, R. K. Wilson, L. Bruhn, M. V. Olson, R. Kaul, D. R. Smith, and E. E. Eichler, “Mapping and sequencing of structural variation from eight human genomes,” *Nature*, vol. 453, pp. 56–64, May 2008.
- [50] T. Marques-Bonet, J. M. Kidd, M. Ventura, T. A. Graves, Z. Cheng, L. W. Hillier, Z. Jiang, C. Baker, R. Malfavon-Borja, L. A. Fulton, C. Alkan, G. Aksay, S. Girirajan, P. Siswara, L. Chen, M. F. Cardone, A. Navarro, E. R. Mardis, R. K. Wilson, and E. E. Eichler, “A burst of segmental duplications in the genome of the African great ape ancestor,” *Nature*, vol. 457, pp. 877–881, Feb 2009.
- [51] A. Soylev, T. Le, H. Amini, C. Alkan, and F. Hormozdiari, “Discovery of tandem and interspersed segmental duplications using high throughput sequencing,” *bioRxiv*, 2018.
- [52] H. Li, “Aligning sequence reads, clone sequences and assembly contigs with BWA-MEM,” *arXiv preprint arXiv:1303.3997*, 2013.
- [53] M. Brunato, H. H. Hoos, and R. Battiti, *On Effectively Finding Maximal Quasi-cliques in Graphs*, pp. 41–55. Berlin, Heidelberg: Springer Berlin Heidelberg, 2008.
- [54] J. C. Mu, M. Mohiyuddin, J. Li, N. Bani Asadi, M. B. Gerstein, A. Abyzov, W. H. Wong, and H. Y. K. Lam, “VarSim: a high-fidelity simulation and validation framework for high-throughput genome sequencing with cancer applications,” *Bioinformatics*, vol. 31, pp. 1469–1471, May 2015.
- [55] R. Luo, F. J. Sedlazeck, C. A. Darby, S. M. Kelly, and M. C. Schatz, “LRSim: a linked-reads simulator generating insights for better genome partitioning,” *Computational and structural biotechnology journal*, vol. 15, pp. 478–484, 2017.

- [56] A. Martínez-Fundichely, S. Casillas, R. Egea, M. Ràmia, A. Barbadilla, L. Pantano, M. Puig, and M. Cáceres, “InvFEST, a database integrating information of polymorphic inversions in the human genome,” *Nucleic Acids Res*, vol. 42, pp. D1027–D1032, Jan 2014.
- [57] J. Huddleston, S. Ranade, M. Malig, F. Antonacci, M. Chaisson, L. Hon, P. H. Sudmant, T. A. Graves, C. Alkan, M. Y. Dennis, R. K. Wilson, S. W. Turner, J. Korlach, and E. E. Eichler, “Reconstructing complex regions of genomes using long-read sequencing technology,” *Genome Res*, vol. 24, pp. 688–696, Apr 2014.
- [58] K. M. Steinberg, V. A. Schneider, T. A. Graves-Lindsay, R. S. Fulton, R. Agarwala, J. Huddleston, S. A. Shiryev, A. Morgulis, U. Surti, W. C. Warren, D. M. Church, E. E. Eichler, and R. K. Wilson, “Single haplotype assembly of the human genome from a hydatidiform mole,” *Genome Res*, vol. 24, pp. 2066–2076, Dec 2014.
- [59] M. J. P. Chaisson, J. Huddleston, M. Y. Dennis, P. H. Sudmant, M. Malig, F. Hormozdiari, F. Antonacci, U. Surti, R. Sandstrom, M. Boitano, J. M. Landolin, J. A. Stamatoyannopoulos, M. W. Hunkapiller, J. Korlach, and E. E. Eichler, “Resolving the complexity of the human genome using single-molecule sequencing,” *Nature*, vol. 517, pp. 608–611, Jan 2015.

# Appendix A

## Glossary

**BAM:** Binary alignment matrix

***nbp:*** *n* base pairs

***nKb:*** *n* kilo base pairs (1000)

***nMb:*** *n* mega base pairs (1,000,000)

**CNV:** Copy Number Variation, variations that change amount of DNA

**DNA:** Deoxyribonucleic Acid, building materials of the genome

**Germline SV:** Structural Variations in the cells that are destined to develop into gametes

**Indel:** Insertions and deletions of size 1 to 50

**Phased Variant:** Variant with a determined haplotype

**SD:** Segmental Duplication, nearly identical sequences in the genome

**SMRT:** Single Molecule Real Time

**SNP:** Single Nucleotide Polymorphism, single nucleotide changes in the DNA

**Somatic SV:** Structural Variations in the cells that are not destined to develop into gametes

**SV:** Structural Variation, changes in the DNA that cover more than 50 bp

**VCF:** Variant Call Format, a format to represent SNPs, indels and SVs

**WGS:** Whole-Genome Shotgun sequencing, sequencing of randomly fragmented sequences

# Appendix B

## Data

The NA12878 genome sequenced with the 10x Genomics Platform is available via the Genome in a Bottle Project FTP site at

<ftp://ftp-trace.ncbi.nlm.nih.gov/giab/ftp/data/NA12878/>

[10Xgenomics\\_ChromiumGenome\\_LongRanger2.1\\_09302016/NA12878\\_hg19/](10Xgenomics_ChromiumGenome_LongRanger2.1_09302016/NA12878_hg19/)

Short read sequencing data for the same genome can be downloaded from the Illumina Platinum Genomes Project at

<https://www.illumina.com/platinumgenomes.html>

The CHM1 genome generated with 10xG Linked-Reads is available at

<https://support.10xgenomics.com/de-novo-assembly/datasets/2.0.0/chm>



# Appendix C

## Code

Implementation is available at <https://github.com/BilkentCompGen/valor>